# Methods for analyzing the concentration and speciation of major and trace elements in marine particles

Phoebe J. Lam[a,*], Benjamin S. Twining[b], Catherine Jeandel[c], Alakendra Roychoudhury[d], Joseph Resing[e], Peter H. Santschi[f], Robert F. Anderson[g]

a-Department of Ocean Sciences, University of California, Santa Cruz, 1156 High St., Santa Cruz, CA 95064. pjlam@ucsc.edu

b-Bigelow Laboratory for Ocean Sciences, 60 Bigelow Dr., East Boothbay, ME 04544, USA. btwining@bigelow.org

c-Observatoire Midi-Pyrénées-14, avenue Edouard Belin-31400-Toulouse-France. Catherine.Jeandel@legos.obs-mip.fr

d- Department of Earth Sciences, Stellenbosch University, Stellenbosch, 7602, South Africa

e-Joint Institute for the Study of the Atmosphere and Ocean, The University of Washington and NOAA-Pacific Marine Environmental Laboratory, 7600 Sand Point Way NE, Seattle, Washington 98115, USA. resing@uw.edu

f- Oceanography And Marine Sciences, Texas A&M University, 200 Seawolf Parkway, Galveston, TX 77553. santschi@tamug.edu

g-Lamont Doherty Earth Observatory of Columbia University PO Box 1000, Palisades NY 10964 USA. boba@ldeo.columbia.edu

* to whom correspondence should be addressed

**Keywords**: marine particles, trace elements, GEOTRACES, particle digestion, leaching methods, synchrotron X-ray fluorescence (SXRF), synchrotron X-ray absorption spectroscopy (XAS)

## Abstract

Particles influence trace element and isotope (TEI) cycles through both their elemental composition and fate and their role on the partitioning of dissolved elements through scavenging and dissolution. Because of their complex compositions, a diverse suite of methods is required to analyze marine particles. Here we review some of the varied approaches used to study particle composition, speciation and fate. We focus on high throughput analytical methods that are useful for the international GEOTRACES program, and we also describe new spectroscopic techniques that are now being applied to study the spatial distribution and chemical speciation of TEIs in marine particles.

## Highlights

- We review methods used to study marine particle composition and speciation
- Multi-element analytical methods are used in GEOTRACES for particle composition
- New X-ray spectroscopic methods are now being applied to marine particles
- Detailed spectroscopic methods are complementary to high-throughput wet chemistry techniques

## 1. Introduction

Particulate matter in the ocean, traditionally defined as materials > 0.2 μm, is one of the main reservoirs for trace elements and isotopes (TEIs), and regulates the distribution of dissolved TEIs through dissolution and scavenging. There is a broad diversity of types and compositions of particulate matter, including intact plankton cells, crustal aluminosilicates, resuspended sediments, authigenic minerals, organic polymers or gels, biogenic detrital material (e.g., fecal pellets, dead cells, empty frustules), or aggregates of a combination of these. In addition, particles in the upper water column can also be generated through

spontaneous aggregation of Dissolved Organic Matter (DOM) into particles termed microgels (Verdugo and Santschi, 2010), ranging from molecules to a typical size of 4 μm, therefore becoming Particulate Organic Matter (POM,Chin et al., 1998). To understand the role of particulate matter in the biogeochemical cycling of both major elements and TEIs in the ocean requires knowledge about both the total composition of suspended matter and the composition of individual particles.

Particles affect TEI cycles both through their elemental composition and through their influence on the scavenging and dissolution of the dissolved elements (Goldberg, 1954; Jeandel et al., this issue; Turekian, 1977). Particle mass and major element composition (such as the proportions of POM, $CaCO_3$, opal, and lithogenic material) may affect the efficiency of the scavenging of several particle-reactive TEIs (Akagi et al., 2011; Chase et al., 2002; Roy-Barman et al., 2005). A number of biopolymers, potentially produced by both phytoplankton and bacteria, could also be carrier molecules for naturally occurring radioisotopes, in addition to the purely inorganic surfaces generally thought to bind radioisotopes (Quigley et al., 2002; Roberts et al., 2009). A greater understanding of the roles of particles often requires the isolation of specific functional groups of particles and sometimes also the determination of the chemical and physical speciation of different elements. For example, the accumulation of TEIs by plankton is a significant control on dissolved metal distributions in the ocean, but determining the TEI content of plankton in natural communities is challenging due to the heterogeneous nature of the particle assemblage (Twining et al., 2008). As another example, the solubility and reactivity of some particle constituents can often be related to the nature of the lithogenic phase(s) that is (are) present (e.g. Si is more reactive in clays than in a grain of quartz; Fe in basalts is mostly reduced and potentially more reactive than oxidized Fe in granites). Thus, determining the mineralogy and speciation of TEIs in the solid phase may be necessary to understand their reactivity. This additional chemical information can also provide clues to the provenance of particles (Lam and Bishop, 2008; von der Heyden et al., 2012).

The complex compositions of marine particles are reflected in their multifaceted role in the cycling of TEIs. To understand these roles, a diverse suite of methods is required to characterize the particles. The methods have to account for relatively dilute concentrations of particles in the ocean and for the trace levels of TEIs in particulate matter. For example, suspended particulate matter (SPM) is typically present at concentrations of only 2-200 μg/kg (Biscaye and Eittreim, 1977; Jeandel et al., this issue). Important bioactive TEIs such as cobalt may be present at ppm levels in biogenic materials, and particulate organic carbon (POC) itself is often present at <10 μM in the open ocean. Thus many particulate TEIs may be present at pM ($10^{-12}$ M) or lower levels in the ocean. While the development of *in situ* optical techniques has enabled the characterization of particle abundance and size spectrum and some estimates of basic particle composition such as POC and particulate inorganic carbon (PIC) concentrations (Boss et al., this issue), the full chemical characterization of particles is essential to understand their role in the biogeochemical cycle of TEIs. Physical sampling of particles and analysis by laboratory-based techniques yield information on particle mass, most major and minor element concentrations, isotopic compositions, and chemical speciation. Sample collection for both major particle composition and TEI analysis is discussed in McDonnell et al. (this issue), Planquette and Sherrell (Planquette and Sherrell, 2012), and Bishop et al. (Bishop et al., 2012).

Here we review some of the varied laboratory-based approaches used to study particle composition. We discuss methods to measure basic particulate parameters that are necessary to understand the role of particles in the cycling of TEIs. Because an understanding of the role of particles in biogeochemical cycling often requires knowledge of the physical and chemical speciation of particles, we also present some of the methods that have been used to

study particle speciation. A review of analytical methods for characterizing marine particles was last published over twenty years ago (Hurd and Spencer, 1991), and many new techniques are now available, particularly spectroscopic techniques.

A comprehensive review of all techniques that can be applied to particles is beyond the scope of this paper. Instead, we aim to provide an overview of methods and touch on some of the major findings that have resulted from these techniques to provide a starting point for further studies. The paper begins with a description of methods to measure major particle composition and suspended particle mass. These are standard techniques that are commonly applied to the analysis of sediment trap material but may not be familiar to the GEOTRACES community. The discussion then shifts to the main focus of this paper, i.e., to the techniques used to measure TEI compositions of particulate matter. These are organized into three categories: 1) analytical or "wet" chemical methods, including chemical leaches of particles, followed by analysis of the solution phase, 2) nuclear techniques, and 3) spectroscopic techniques, in which the interaction of radiation with matter is used to determine elemental composition, mineralogy, or chemical speciation in the solid phase.

## 2. Major particle composition and suspended particle mass

The mass of total suspended matter in the ocean is the sum of its major, minor, and trace components, however it depends mostly upon its major components, which include particulate organic matter, biogenic silica, calcium carbonate, and often also lithogenic matter, strontium and barium sulphate, and iron and manganese oxyhydroxides. The major particle phases are implicated in the control of particle flux to depth (François et al., 2002; Klaas and Archer, 2002) and of scavenging of particle-reactive TEIs (Akagi et al., 2011; Chase et al., 2002; Roy-Barman et al., 2005). The total mass of suspended particulates is one basic measurable parameter that enables greater understanding of the role that particles play in the cycling of many TEIs. Gravimetric methods are the most direct way to determine the dry weight of marine particulate matter, but it is critical to remove sea salt before it crystallizes (e.g., Karageorgis et al., 2008), or to correct for the mass contribution of salt (Bishop, 1991). The complete removal of sea salt is not always possible, however, especially with the high-throughput filter types used with in-situ pumps that retain excess seawater. Because the correction for sea salt is not trivial (Lam and Bishop, 2007), an alternative method is to determine the "chemical dry weight" of particles (e.g., Bishop et al., 1977), which is the sum of the masses of the major particle components determined separately.

The determination of all major particle components typically requires the collection of particles onto at least two filter types (McDonnell et al., this issue), usually a pre-combusted glass or quartz-fiber filter for particulate organic matter, and a carbon-based filter for biogenic Si and lithogenic material. Particles collected from sampling bottles (e.g., Niskin) can be filtered onto two filter types by using multiple bottles tripped at the same depth, but this may reduce the volume available for each sample. In-situ filtration provides an alternative method to sample significantly larger volumes. Collection of particles for major particle composition by in-situ filtration is ideally accomplished using a pump that has at least two flow paths (e.g., Bishop et al., 1985; Lam and Morris, Patent pending) so that particles can be collected simultaneously on two filter types.

Standard methods for determining each component can be used. Briefly, POC is determined by combustion (e.g., http://usjgofs.whoi.edu/eqpac-docs/proto-18.html) and converted to POM using a POM/POC ratio ranging from 1.88 g/g (Timothy et al., 2003) to 2.5 g/g (Bishop et al., 1977), depending on the assumed molecular formula for POM. Biogenic silica is typically determined by a weak alkaline leach followed by spectrophotometric detection (e.g., Mortlock and Froelich, 1989), and sometimes with correction for the contribution of lithogenic Si in oceanic regions of high lithogenic Si/biogenic Si (DeMaster,

1981; Ragueneau et al., 2005), and then converted to opal mass assuming a hydrated form of silica (e.g., $SiO_2.(0.4\ H_2O)$) (Mortlock and Froelich, 1989). $CaCO_3$ is determined by coulometric detection of $CO_2$ following addition of acid (e.g., Honjo et al., 1995), or from Ca following correction of Ca from sea salt (e.g., Lam and Bishop, 2007). Lithogenic material is determined by measuring the concentration of a lithogenic tracer such as Al or Ti, and scaling up to a crustal mass using average crustal abundances (e.g., Honjo et al., 1995). $SrSO_4$ is determined from salt-corrected Sr (Bishop et al., 1977). Finally Fe and Mn oxyhydroxides are estimated from Fe and Mn following a weak acid leach or from total Fe and Mn that has been corrected for lithogenic Fe and Mn (such as by using Ti as a lithogenic tracer) (Lam et al., in press; Ohnemus and Lam, in press).

For example, on the US GEOTRACES North Atlantic Zonal Transect (GA03), the chemical dry weight of particles was determined as (Lam et al., in press):

$$\text{SPM (g)} = \text{POM} + \text{opal} + CaCO_3 + \text{lithogenic} + Fe(OH)_3 + MnO_2 \quad (1)$$

where

$$\text{POM} = \text{POC (g)} * 1.88\ \text{(g POM/g POC)} \quad (2)$$

$$\text{opal} = \text{bSi (mol)} * 67.2\ \text{(g opal/mol bSi)} \quad (3)$$

$$CaCO_3 = \text{Ca (mol)} * 100.08\ (\text{g } CaCO_3\text{/mol Ca}) \quad (4)$$

$$\text{Lithogenic} = \text{Al (g)} / 0.0804\ \text{(g Al/g crust)} \quad (5)$$

$$Fe(OH)_3 = (\text{Fe (mol)} - \text{Ti (mol)} * 8.7\ \text{(mol Fe/mol Ti)}) * 106.9\ \text{g } Fe(OH)_3\text{/mol Fe} \quad (6)$$

$$MnO_2 = (\text{Mn (mol)} - \text{Ti (mol)} * 0.13\ \text{(mol Mn/mol Ti)}) * 86.9\ \text{g } MnO_2\text{/mol Mn} \quad (7)$$

The effect of particle composition on scavenging efficiency has so far mostly been studied using particle-reactive long-lived radionuclides such as $^{230}Th$ in the field (Chase et al., 2002; Roy-Barman et al., 2005), and $^{234}Th$, $^{233}Pa$, $^{210}Pb$, $^{210}Po$, and $^{7}Be$ in laboratory tracer studies with field-collected or cultured particles (Chuang et al., 2013; Chuang et al., 2014; Roberts et al., 2009). The GEOTRACES program provides the opportunity to greatly expand our understanding of the role of particle concentration and composition on the scavenging of a broader suite of particle-reactive TEIs.

## 3. Particulate TEI composition

### *3.1 Analytical ("wet") chemistry techniques to measure particulate TEIs*

#### *3.1.1 Total chemical digests*

Although an extensive literature describes the chemical digestion (complete and sequential) of sediments, the digestion of marine suspended particles collected on filters presents additional challenges. Particulate TEIs were traditionally collected on polycarbonate membrane filters because of their low blanks (e.g., Cullen and Sherrell, 1999; Landing and Bruland, 1987; Sherrell and Boyle, 1992). However, because polycarbonate-membrane filters have relatively low sample throughput, and the larger diameter sizes (e.g., 142 mm or 293 mm) used for in-situ filtration are difficult to handle, many GEOTRACES programs are using polyethersulfone filters (e.g., Supor) due to their low blanks, ease of handling, and high volume throughput (Bishop et al., 2012; Planquette and Sherrell, 2012). Supor filters are, however, very difficult to digest. One strategy is to employ a refluxing method in which the filter piece is not submerged in the strong acid, thus leaving it intact (Planquette and Sherrell, 2012), but this method is only suitable for relatively small pieces of filter. Most heated strong acid digestions of submerged filters will break Supor filters down partially without achieving a complete dissolution. The cooled solution must often then be filtered to remove undigested filter pieces that may cause clogging of subsequent analytical steps. Complete dissolution of Supor filters can be achieved using strong oxidizing acids such as perchloric acid (Anderson

et al., 2012) or Piranha solution, which is a 3:1 mixture of concentrated sulfuric acid and 30% hydrogen peroxide (Ohnemus et al., 2014). It may also be possible to achieve complete dissolution of Supor filters using nitric acid or aqua regia at elevated temperature and pressure using microwave systems (L. Robinson, pers. comm.; S. Severmann, pers. comm.) or wet ashers (T. Horner, pers. comm.). Since the strong oxidizing acids that dissolve the filter do not dissolve silicates, the filter dissolution step is usually followed by the digestion of the collected particulate material using hydrofluoric acid in combination with nitric and (or) hydrochloric acid (e.g., Anderson et al., 2012; Ohnemus et al., 2014).

*3.1.2 Selective chemical leaches*

There is a long history of applying selective chemical washes and leaches to attempt to isolate specific components from the heterogeneous mixture that comprise natural particulate materials (e.g., Chester and Hughes, 1967; Tessier et al., 1979), and an equally long history of criticisms of these methods (e.g., Kheboian and Bauer, 1987; Nirel and Morel, 1990; Sholkovitz, 1989). At the heart of the controversy is whether selective leaches are extracting a scientifically meaningful fraction from a given heterogenous particulate phase, and, if they are, whether the leaching of these fractions is quantitative and reproducible between research laboratories. Failure to achieve quantitative recovery might occur, for example, if mobilized species are re-adsorbed by refractory solid phases. Despite these controversies, leaches are still actively used since they provide a quick and high-throughput method for operationally assessing differences in the lability of given phases within in a sample set, which likely reflects underlying chemical differences.

The number of leaches in existence is almost endless, and new ones are continually being developed, particularly in the soil and sediment communities, that attempt to optimize conditions for specific TEIs, sample types, and scientific questions. As a result, there is no ideal leach that is applicable to all TEIs, and one must refer to the literature of one's specific field. A few that have been used to determine the trace metal concentration in suspended particles are mentioned below.

Collier and Edmond (1984) subjected suspended marine particles collected using plankton nets to a wide range of sequential chemical leaches, focusing on the weakly adsorbed and biogenic fractions. Their experiments showed that many elements were very weakly associated with plankton and rapidly released into seawater. In general, however, multi-step sequential leaches have not typically been applied to suspended marine particles because of limitations in sample size. The phases identified by most leaches that have been applied to suspended marine particles have been operationally defined. For example, "acid-leachable" concentrations of particulate trace metals have been reported for particles following a 25% acetic acid leach (e.g., Landing and Bruland, 1987) or a 0.6 M HCl leach (e.g., Lam and Bishop, 2008) and compared to total concentrations determined by strong acid digestion including HF or by other methods such as X-ray fluorescence. More recently, a modification of the acetic acid leach has been developed to access a "labile-biogenic" fraction (Berger et al., 2008), and washes have been developed that attempt to separate a loosely-bound, extracellular fraction from an intracellular fraction (Tang and Morel, 2006; Tovar-Sanchez et al., 2003), although the utility of this latter leach for heterogeneous particle samples has been disputed (Twining and Baines, 2013). Despite the continuing debates about the merits of individual leaches, they remain an important tool for assessing broad differences in the lability and thus chemical composition of particles, as long as one acknowledges the caveats associated with using them.

*3.1.3 Analysis of particle leaches and digests*

In the past, total digest solutions and leachates were typically analyzed using Atomic Absorption Spectroscopy (AAS), which allows the measurement of one TEI per analysis. Early results from AAS include the publication of the first particulate barite profiles, for example, that allowed the understanding of the link between barite precipitation and biological production and decay of organic matter in the water column (Bishop, 1988; Dehairs et al., 1980). Those studies led to the development of barite in sediments as a paleo-productivity proxy (Dymond et al., 1992). The first data on the trace metal composition of phytoplankton collected by nets were also generated using AAS (Collier and Edmond, 1984; Martin and Knauer, 1973). These showed that the carrier phase for many trace elements was non-skeletal organic matter (Collier and Edmond, 1984). It was also noted that elements such as Al, Fe, and Ti were found largely in the refractory phase, suggesting that terrigenous (lithogenic) particles were present even in remote regions. The first full ocean-depth profiles of multiple particulate trace metals were also produced with AAS (Sherrell and Boyle, 1992). These authors found that the shapes of the particulate Co, Pb, Zn, Cu, and Ni profiles were similar to that of particulate Mn, and postulated that Mn oxyhydroxides might play an important role in scavenging trace metals. Indeed, Mn oxyhydroxides have also been hypothesized to control the scavenging of long-lived radionuclides such as $^{230}$Th in the Northeast Atlantic and Mediterranean Sea (Roy-Barman et al., 2005). The overall importance of Mn oxyhydroxides for controlling the scavenging of particle-reactive TEIs needs to be tested with more data, such as will be generated during the GEOTRACES program.

The development of plasma systems (producing excited atoms and ions) coupled to either an optical detector (Inductively Coupled Plasma Atomic Emission Spectroscopy, ICP-AES) or a mass spectrometer (ICP-MS, some including high resolution mass discrimination) has considerably improved detection limits, precision, as well as analyte and sample throughput for natural sample analysis (Bowie et al., 2010; Cullen et al., 2001; Ho et al., 2011; Ho et al., 2010; Ho et al., 2007; Kuss and Kremling, 1999). Analytical constraints and instrumental operating parameters for multi-element analysis have been described for ICP-AES by Sandroni and Smith (2002), and for ICP-MS by Bowie et al. (2010), Cullen et al. (2001), Feldmann et al. (1994), and Linge and Jarvis (2009).

Thanks to the development of ICP-related instrumentation, Kuss and Kremling (1999) were the first to establish the distribution of multiple particulate TEIs on the ocean basin scale. They determined 10 particulate trace elements, POC, opal, and $CaCO_3$ from 24 near-surface samples in the North Atlantic, and showed that variability in particle composition could be explained by the changing importance of biological production, different water masses of the North Atlantic Current system, and atmospheric dust deposition, particularly in the trade wind area off Africa. Close to the Asian continent, Ho et al. (2007) showed that particulate trace metals associated with phytoplankton in the South China Sea were largely derived from anthropogenic aerosols, and that these were removed from the water column via the rapid sinking of biogenic particles (Ho et al., 2011; Ho et al., 2010). The increase in studies reporting multi-element particulate trace metal concentrations in different ocean basins is opening up many perspectives in the role of particles in the cycling of both micronutrient and toxic trace metals from natural and anthropogenic sources.

### *3.2 Nuclear techniques to measure particulate TEIs*

Although Instrumental Neutron Activation Analysis (INAA) has not been widely used because it requires access to a high-flux neutron source, it was employed in the early investigations of the trace element composition of marine particles because it offered multi-element analysis with sufficient sensitivity to produce useful results with relatively small samples (tens to hundreds of micrograms dry weight of particulate material). Neutron bombardment of the sample causes element-specific radioactive emissions, which are

measured. INAA also offered the advantage of requiring little or no chemical preparation of samples other than removing sea salt from filters before activation. The method has been applied successfully to particles collected both by filtration (e.g., Fleer and Bacon, 1991; Spencer et al., 1972) and by sediment traps (e.g., Brewer et al., 1980; Deuser et al., 1981; Spencer et al., 1978). These early studies of the sinking flux of major and minor elements showed that particle settling velocities were considerably higher than previously expected. Moreover, the flux of all major and minor elements, even those not thought to be biological, demonstrated seasonality that followed the annual cycle of primary production. This showed that the vertical flux of biological matter was an efficient mechanism to scavenge and remove many chemicals from the water column. The advent of ICP-MS for multi-element analysis of marine particles has mostly eliminated analyses by INAA, although it is still finding use in research on the composition of aerosols (e.g., Almeida et al., 2013; Steinnes, 2000).

### *3.3 X-Ray Diffraction (XRD)*

XRD is a rapid analytical technique used for phase identification of a crystalline material. Monochromatic X-rays are directed at the sample and the diffracted X-rays are collected. The wavelength of X-ray radiation is related to the diffraction angle and the lattice spacing (d-spacing) in a crystalline sample (Bragg's law). Conversion of the diffraction peaks to d-spacings allows identification of the mineral by comparison of d-spacings with standard reference patterns. Both bench-top and synchrotron-based XRD techniques are used. Prior to analysis by bench-top XRD, a sediment or soil sample is finely ground, homogenized, and average bulk composition is determined. Particulate material has to be removed from the filter (hence polycarbonate membranes recommended) and be relatively abundant, which might restrict this method to coastal samples. However, XRD can now also be conducted at some synchrotron beamlines (Tamura et al., 2002), which removes the requirement for sample homogenization, reduces sample size requirements, and allows the targeting of micron-scale areas of interest. For example, $CaCO_3$ in the form of the mineral ikaite ($CaCO_3.6H_2O$) was discovered in Antarctic sea-ice for the first time using synchrotron XRD (Dieckmann et al., 2008). This abiotic precipitation of $CaCO_3$ in sea ice brine may have implications for carbon cycling in seasonally sea ice-covered regions (Bates and Mathis, 2009). Micro-focused synchrotron XRD has been used to determine the mineralogy of micron-thick Fe-rich and Mn-rich layers of ferromanganese nodules (Marcus et al., 2004) and the mineralogical structure of Fe-encrusted biofilms at mid-ocean ridge hydrothermal vents (Toner et al., 2009b), both of which aid in the understanding of their formation conditions, as well as their roles for the scavenging of other trace metals.

### *3.4 X-ray based spectroscopic techniques to measure particulate TEIs*

Spectroscopic techniques encompass a wide range of approaches that are all related by their use of the interaction of electromagnetic radiation and matter in the solid phase. We focus here on X-ray based spectroscopic techniques, and do not discuss other types of spectroscopies (e.g., Infrared (FTIR) or ultra-violet (RAMAN)) that have also been useful for environmental samples. There are many books and papers that review the principles of X-ray theory (Bunker, 2010; Conradson, 1998; Koningsberger and Prins, 1988; Teo, 1986) and applications to environmental samples (Fenter et al., 2002; Kelly et al., 2008; Parsons et al., 2002). Here, we provide a brief overview and point to techniques that have applications for marine particulate samples.

The X-ray based spectroscopic techniques involve electronic rather than nuclear transitions (Section 3.2). They are united by requiring X-rays or high-energy beams of charged particles to induce an electronic transition, and the detection of resultant emitted X-rays or particles. X-rays are used to induce electronic transitions for X-Ray Fluorescence

(XRF), X-Ray Photoelectron Spectroscopy (XPS), X-ray Absorption Spectroscopy (XAS), and Scanning Transmission X-ray Microscopy (STXM); an electron beam is used to induce the transition for Scanning Electron Microscopy-Energy Dispersive X-ray Spectroscopy (SEM-EDS). With the exception of XPS, in which emitted electrons are detected, the other techniques measure absorbed (XAS, STXM) or emitted (XRF, SEM-EDS) X-rays to determine composition. We summarize some of the essential characteristics of these X-ray based spectroscopic techniques in Table 1.

The methods can be characterized by those that measure elemental concentrations (XRF, XPS, SEM-EDS), and those that measure chemical speciation and bonding structure (XPS, XAS, STXM). Collection of particles for spectroscopic analyses of TEIs should follow trace-metal clean techniques (McDonnell et al., this issue). Most of the above techniques can be performed in bulk mode, in which the average concentration or speciation of a particle assemblage is determined over a several millimeter area, or in a micro- or nano-focused mode, which allows particle-by-particle analysis and mapping of the distribution of elements and chemical species at the micron or even sub-micron level. Some of these techniques, such as laboratory-based XRF, have been employed in the analysis of marine suspended particles for two to three decades (e.g., Feely et al., 1991a); others, such as synchrotron-based XRF and XAS, have been used for the analysis of soils and sediments for several decades, but have only been applied to the analysis of suspended marine particles in the last decade (e.g., Lam et al., 2006; Toner et al., 2012b; Twining et al., 2003). Many of the mapping and speciation techniques are relatively time-intensive, and so are best suited for detailed characterization of a subset of samples to complement bulk geochemical distributions determined by higher throughput wet analytical techniques (Section 3.1).

### *3.4.1 Scanning Electron Microscopy-Energy Dispersive X-ray Spectroscopy (SEM-EDS)*

In this technique a scanning electron microscope (SEM) produces a focused beam of high-energy electrons to generate a variety of signals at the surface of solid specimens. Re-emitted electrons from the sample allow identification of the external morphology, and fluorescent X-rays generated by the electrons can also be quantified by an energy dispersive detector (EDS) to determine the qualitative or semi-quantitative chemical compositions of materials composing the sample (Goldstein et al., 2003). Marine particles to be analyzed by SEM-EDS must be collected on polycarbonate membranes and sea salt needs to be removed prior to analysis. Data are collected over a selected area (typically 5 μm to 1 cm width) of the surface of the sample, and a 2-dimensional image is generated. Among the re-emitted signals, EDS is used to separate the characteristic X-rays of different elements into an energy spectrum, which is analyzed in order to determine the abundance of specific elements and allowing for the the generation of elemental composition maps (e.g., Resing et al., 2007). These capabilities provide major elemental compositional information for a wide variety of materials (Heldal et al., 2003). SEM-EDS coupled with automated analysis was successfully applied to determine the composition of hundreds to thousands of particles from the nepheloid layers from the GEOSECS Atlantic program (Bishop and Biscaye, 1982) and from the water column in the Sargasso Sea (Lavoie, 1992). It has also been used to directly determine the barite concentration on filtered material with satisfying comparison with chemical analysis (Sternberg et al., 2008) using a method developed by Robin et al. (2003). Seasonal distribution of barite in the water column of the NW Mediterranean Sea was documented with this method (Sternberg et al., 2008). SEM-EDS is less sensitive to transition and heavy metals due to significant background Bremsstrahlung (Heldal et al., 1996), which is radiation produced by the deceleration of charged particles such as electrons.

### *3.4.2 X-Ray Fluorescence (XRF)*

In laboratory- and synchrotron-based XRF, the incident X-ray is absorbed by atoms in the sample, ejecting core electrons. An electron from an outer shell fills the hole, leading to the emission of a fluorescent X-ray of well-defined energy (Figure 1), whose intensity is measured with a detector that is placed orthogonal to the incident radiation. The energy of the fluorescent X-ray is element-specific, and its intensity depends on the concentration of the element. Thus, the identities and concentrations of multiple elements can be determined.

#### *3.4.2.1 Energy-Dispersive X-Ray Fluorescence (ED-XRF)*

ED-XRF is a laboratory-based XRF technique that allows for the non-destructive chemical analysis of marine particles (Baker and Piper, 1976; Feely et al., 1991a). Suspended particulate matter is deposited onto a polycarbonate membrane filter as a thin film. This film is irradiated with X-rays, which in turn induce individual elements within the particle film to fluoresce at energies characteristic of each element. This method follows principles similar to that of SEM-EDS, although bench-top generated X-rays are used instead of electrons to generate fluorescence X-rays. This technique is capable of quantifying most elements with atomic number greater than 11, and analysis of Mg, Al, Si, P, S, K, Ca, Ti, V, Cr, Fe, Ni, Cu, Zn, As, Sr, and Pb has been demonstrated for marine suspended particulate matter (Barrett et al., 2012). Sample collection is usually made by passing seawater directly from a sampling bottle through a filter that is supported by an in-line filter holder (see McDonnell et al., this issue). Once collected, the filter membrane is rinsed with a small volume of pH 8 de-ionized water and stored in a petri-dish within a desiccated environment. The dried sample is then analyzed by ED-XRF. Sample films deposited onto membranes must meet two criteria. First, particles must be deposited as a uniform layer or film. Second, the thickness of the film must be thin relative to both the penetration depth of the primary X-ray and the depth from which the fluorescent X-rays emerge (Bertin, 1975; Criss, 1976; Dzubay and Nelson, 1975). ED-XRF instrumentation can be calibrated using commercially available thin-film standards (Micromatter Inc,) and (or) using standards fabricated using a variation of a sodium-diethyl-dithio-carbamate pre-concentration method (Hołyńska and Bisiniek, 1976).

The ED-XRF technique has been used successfully since the mid 1980s to document the distribution and unique chemistries associated with hydrothermal venting in a variety of submarine volcanic settings (Feely et al., 1991a). The chemical composition of total suspended matter in hydrothermal plumes at mid-ocean ridges reveals the formation of Mn- and Fe-oxhydroxides (Cowen et al., 1990) and their roles in scavenging P, V, and As from seawater (e.g., Feely et al., 1998; Feely et al., 1991b), thus demonstrating that hydrothermal activity results in the net removal of these species from sea water. The Fe:P and Fe:V ratios in these plume samples are a function of the ambient phosphate concentration in the local ocean environment, suggesting a possible paleo-indicator of oceanic phosphate concentrations. More recently the technique has been applied to suspended particulate matter from the open ocean (Barrett et al., 2012) and to aerosols collected in the marine atmospheric boundary layer (Buck et al., 2013; Buck et al., 2010a; Buck et al., 2006; Buck et al., 2010b; Ranville et al., 2010). These studies reveal the dominant impacts of aerosol deposition to the ocean on the dissolved and particulate TEI chemistry in the Atlantic and Pacific Oceans.

#### *3.4.2.2 Synchrotron based X-Ray Fluorescence* (SXRF)

SXRF techniques provide the ability to quantitatively map the distribution of elements at sub-micron to millimeter spatial scales. Again, fluorescence X-rays are generated, but using the power and brilliance of synchrotron X-rays instead of bench-top generated X-rays (as in ED-XRF or XPS) or electrons (as in SEM-EDS) to obtain adequate sensitivity when the incident beam is focused to micron- and sub-micron areas.

Comparisons of SXRF with standard bulk techniques have shown this approach to produce comparable results for biogenic TEIs (Mn, Fe, Ni, Zn) and biomass elements P and Si (Núnez-Milland et al., 2010; Twining et al., 2004b; Twining et al., 2003) in identical samples. However, application of SXRF to measure cellular metal quotas alongside ICP-MS measurements of bulk particulate element concentrations in natural systems has shown that these approaches provide different information. Bulk particulate Fe concentrations (normalized to the biomass proxy P) are typically higher than co-occurring cellular Fe:P ratios due to the inclusion of lithogenic and detrital particles that are relatively rich in Fe (King et al., 2012; Twining et al., 2011; Twining et al., 2004b). In certain cases analyses can be expanded to include minor trace metal constituents such as Co and V (Nuester et al., 2012). Using this approach, significant spatial, temporal and taxonomic variations in the TEI content of naturally-occurring phytoplankton have been measured (Twining and Baines, 2013; Twining et al., 2011; Twining et al., 2004a; Twining et al., 2010). For example, Fe, Ni and Zn contents of cyanobacteria from neighboring mesoscale eddies in the Sargasso Sea can vary by more than an order of magnitude as a result of different nutrient inputs (Twining et al., 2010), while in the equatorial Pacific Ocean metal quotas of eukaryotic phytoplankton vary across and along the equator, due to both upwelling and the passage of tropical instability waves (Twining et al., 2011). SXRF-produced maps of sub-cellular TEI distributions are also valuable, suggesting physiological uses for metals (Nuester et al., 2014) as well as the internal and external associations of metals with cells in some cases (Núnez-Milland et al., 2010; Twining et al., 2004b; Twining et al., 2003).

Coarser-scale SXRF mapping of size-fractionated suspended particulate or sediment trap samples on filters can reveal the larger-scale systematic behaviors of different TEIs. For example, the often-dominant lithogenic and authigenic components of elements such as Fe and Mn are manifested as intense micron-sized Fe and Mn hotspots (pixels with very high count rates) above the much lower biogenic background. Indeed, abundant micron-sized Fe-rich particles detected by SXRF in subsurface marine particles were the primary indication of the importance of lateral transport of Fe from the continental margin to the open Subarctic Pacific (Lam et al., 2006). In contrast to particulate Fe and Mn distributions in hotspots, TEIs such as Zn that have a much larger biogenic component are distributed evenly with biogenic matter (Lamborg et al., 2008). The spatial distribution of trace elements in single particles and particle aggregates that can be inferred by SXRF adds a new perspective to previous bulk determinations of particulate trace metal concentrations.

*3.4.3 X-ray Absorption Spectroscopy (XAS)*

For measurements of chemical speciation, the absorption of X-rays by a sample is measured as a function of incident energy. XAS techniques differ to XRD in that they are element-specific and do not require chemical structural order. This makes XAS suitable for characterizing trace elements that are poorly (or not) crystalline. X-ray absorption is a function of sample thickness and the X-ray absorption coefficient ($\mu$), which is the probability for an X-ray to be absorbed by a sample (Kelly et al., 2008).

The probability of X-ray absorption depends strongly on atomic number and incident energy, as well as the local bonding environment of the target atom, providing information about the chemical speciation of the sample (Kelly et al., 2008; Sham and Rivers, 2002). All XAS techniques include collection of data at the absorption "edge", which is a term used to describe the rapid increase in the absorption of X-ray photons at the energy just above the binding energy of the electrons associated with the atoms being probed by the incident X-rays (Figure 2). At energies above the absorption edge, core electrons are ejected from the atom, where they are called photoelectrons.

Electrons are contained within shells corresponding to the principle quantum numbers (e.g., 1, 2, 3…). By convention in X-ray physics, the shells are labelled with letters: K (1st shell), L (2nd shell), M (3rd shell). The K-edge therefore corresponds to the absorption of X-rays by electrons in the 1s sub-shell, and the $L_2L_3$ edge corresponds to the absorption of X-rays by electrons in the $2p_{1/2}$ and $2p_{3/2}$ sub-shells, where the subscripts denote the total angular momentum quantum number. The energies of the absorption edges are unique to each element and each sub-shell. The K-edge is always at higher energy than the L-edge for a particular element, and the energies of K- and L-edges increase as a function of atomic number. For example, the carbon K-edge for elemental carbon occurs at 284 eV, while the K, $L_2$, and $L_3$ edges for elemental iron occur at 7112 eV, 720 eV, and 707 eV, respectively. Example absorption spectra for iron at the $L_3$- and K-edges are shown in Figure 2. Because each absorption edge is the result of different electronic transitions, the information gained also differs slightly, but the principle remains the same.

When the incident radiation is in the soft X-ray energy range (< 2 keV) or for particularly concentrated samples in the hard X-ray energy range (> 5 keV), the absorption of incident radiation can be directly measured using a detector that is placed behind the sample in the X-ray path. The X-ray absorption coefficient is derived from the measured X-ray intensities in front of and behind the sample (Kelly et al., 2008). Since X-ray fluorescence results from and is proportional to the absorption of X-rays (Section 3.4.2), measuring the emitted X-ray fluorescence is an alternative and more sensitive method for detecting X-ray absorption for dilute samples. When using fluorescence, the fluorescence detector is placed at right angles to the incident radiation to minimize the intensity of scattered X-rays from the incident beam (Kelly et al., 2008; Parsons et al., 2002).

*3.4.3.1 XANES, NEXAFS, and EXAFS*

The region of the X-ray absorption spectrum around the absorption edge is referred to as the X-ray Absorption Near Edge Structure (XANES) region, also called the Near Edge X-ray Absorption Fine Structure (NEXAFS) (Figure 2). The position (energy) of the edge is a function of the oxidation state of the element of interest. At incident X-ray energies above the absorption edge, the absorption of X-rays leads to the ejection of a photoelectron that is then backscattered from surrounding atoms, modulating the absorption probability of incident X-rays. This is because the absorption of X-rays by a core election is only possible if there is an available state for the photo-electron to transition to. The presence of a backscattered photo-electron wave alters the probability of this, thus modulating the absorption coefficient (Newville, 2004). The resulting oscillations in the absorption coefficient in the higher energy Extended X-ray Absorption Fine Structure (EXAFS) region are measured, and are related to the average distances, identity, and number of coordinating atoms.

While both XANES and EXAFS analyses provide information about the local bonding environment of the central absorbing atom, there are some key theoretical and practical differences between the two. The most important practical difference is that collection of XANES data typically takes minutes for environmental samples, whereas collection of EXAFS data typically takes hours. XANES data are excellent for determining the oxidation state of the element of interest (e.g., Wilke et al., 2001), and are often sufficient for distinguishing between major groups of minerals (e.g., oxyhydroxides versus sulfides) (e.g., Lam et al., 2012; Toner et al., 2014), but may not be able to distinguish between more closely related species (e.g., different forms of oxyhydroxides), for which EXAFS may be required (e.g., Manceau and Drits, 1993; Toner et al., 2009b).

A variety of empirical methods have been developed to extract oxidation state and crude mineralogical information from the position and size of the features at the L-edge (e.g., von der Heyden et al., 2014; von der Heyden et al., 2012) and K-edge (e.g., Marcus et al.,

2008; Wilke et al., 2001). Extending the collection of XANES data several hundred eV above the main edge additionally facilitates the quantitative analysis of unknown XANES spectra by linear combination fitting using a library of reference materials (Kelly et al., 2008). The theoretical basis of oscillations in the EXAFS range is well understood, so the equation describing EXAFS oscillations can be solved from first principles for the number and identity of neighboring atoms, the distance to the neighboring atom, and the disorder in the neighbor distance (Bunker, 2010; Koningsberger and Prins, 1988). Alternatively, EXAFS spectra can also be quantitatively analyzed by linear combination fitting. There are several freely available software packages to analyze XANES and EXAFS data (e.g., Marcus, 2011; Ravel and Newville, 2005; Webb, 2005). The details of XAS data analysis are beyond the scope of this paper, but we refer the reader to the many excellent online tutorials (e.g., http://xafs.org/Tutorials), papers (e.g., Conradson, 1998; Kelly et al., 2008; Parsons et al., 2002), and books (e.g., Bunker, 2010; Fenter et al., 2002; Koningsberger and Prins, 1988; Teo, 1986) that exist on EXAFS theory and applications.

*3.4.3.2 Scanning Transmission X-ray Microscopy (STXM)*

STXM is a spectromicroscopy technique that combines the high resolution of an X-ray microscope with some of the spectroscopic information of NEXAFS (Bluhm et al., 2006). It operates in the soft (lower energy) X-ray range (~100-2000 eV), which has lower penetration than a hard X-ray microprobe and so can only be applied to very thin samples. One of its primary advantages is that it can produce maps detailing elemental associations and chemical speciation at very high spatial resolution (tens of nanometers), provided the elements of interest have an appropriate absorption edge in the STXM energy range. The STXM energy range encompasses both the carbon K-edge and the iron L-edge, permitting the determination of organic matter functional groups (e.g., Brandes et al., 2004; Lehmann et al., 2009), some of which may be binding Fe (Toner et al., 2009a; von der Heyden et al., 2014). For STXM, particles must be removed from the filter on which they were collected, washed of sea salt, and placed onto an X-ray transparent substrate.

*3.4.3.3 Applications of XAS to marine particle cycling*

Particulate iron has thus far received the most attention by XAS techniques in the marine community because of its relatively high concentration in suspended particulate matter, particularly near continental margins and hydrothermal vents, but particulate C and S speciation in suspended marine particles have also been reported using these techniques (Breier et al., 2012; Lam and Bishop, 2008; Lam et al., 2006; Lam et al., 2012; Toner et al., 2009a; Toner et al., 2012b; von der Heyden et al., 2012).

Iron is typically analyzed either at the K- or $L_3$-edge (see Figure 2). XANES and EXAFS at the K-edge have been applied for the determination of the local coordination environment at the iron site in metalloproteins such as cyanobacterial ferritin (e.g., Castruita et al., 2006), model complexes (e.g., Duckworth et al., 2008), and minerals (Lam and Bishop, 2008; Lam et al., 2012; Toner et al., 2012a; Toner et al., 2009b; Waychunas et al., 1986). A hard X-ray microprobe performing microfocused XANES (μXANES) and EXAFS (μEXAFS) spectroscopy can provide detailed mineralogical information of individual particles at the micron-scale (e.g., Ingall et al., 2013; Lam et al., 2006). The related chemical species mapping technique allows rapid identification of minor species that would never be identified by bulk techniques (Lam et al., 2012; Toner et al., 2012b; Toner et al., 2014). These studies have shown the high heterogeneity in the speciation of marine particulate iron, including poorly crystalline Fe(III) compounds such as oxyhydroxides and clays, Fe sulfides, and Fe(II) silicate minerals, and have implications for the solubility and bioavailability of different forms of particulate iron.

The Fe L-edge has been less utilized, although it can provide more detailed electronic information (Wasinger et al., 2003). Because it is typically conducted on STXM beamlines that have much higher spatial resolution, this allows smaller, colloidal particles to be probed (e.g., Toner et al., 2009a; von der Heyden et al., 2014; von der Heyden et al., 2012). Using STXM, persistent particulate Fe(II) has been found associated with particulate organic carbon in both hydrothermal plumes (Toner et al., 2009a) and oxygenated euphotic zones (von der Heyden et al., 2012), raising questions about our understanding about the presumed stability of reduced forms of iron in oxygenated seawater.

The speciation of mineral Fe can also be used as a tracer for the provenance of Fe to iron limited open ocean regions (Lam and Bishop, 2008; Lam et al., 2006; Lam et al., 2012; von der Heyden et al., 2012). For example, the abundance of crystalline Fe(II) minerals in subsurface waters of the Western Subarctic Pacific suggested a source from the surrounding volcanic margin, demonstrating the importance of lateral transport of Fe over many hundreds of kilometres (Lam and Bishop, 2008).

*3.4.4 X-ray Photoelectron Spectroscopy (XPS)*

X-ray Photoelectron Spectroscopy (XPS) follows the same physical principles as XAS (Behra et al., 2001; Brown Jr and Calas, 2012), and can use a bench-top or synchrotron X-ray source to illuminate the sample. The energy difference between the incidental beam and the kinetic energy of the electron beam ejected by the sample allows the description of the elemental concentration (in parts per thousand range) and the speciation within the first 10 nm of the solid surface. Unlike XAS, which can be used on liquid and colloidal samples, XPS analysis is restricted to samples in the solid form and under high vacuum, but is well adapted to the study of surface physico-chemistry.

## 4. Conclusions

In this paper, we have reviewed techniques that are used to study the composition and speciation of marine particles. The analytical « wet » chemistry techniques described here are being used in a high-throughput fashion to measure the first full ocean depth, basin-wide sections of marine particulate distribution and composition as part of the international GEOTRACES program (Lam et al., in press; Ohnemus and Lam, in press; Twining et al., in press). We also described the physical principles behind spectroscopic techniques that may not be as familiar to the oceanographic community. Some of these spectroscopic techniques are already being used on select samples in GEOTRACES to complement high-throughput analytical techniques, such as the speciation of particulate iron in oxygen minimum zones and hydrothermal vents using XAS, and the trace metal quotas of phytoplankton using SXRF. This pairing has enormous potential to unveil new discoveries about particles and their role in the cycling of TEIs.

## Acknowledgements

This paper arose from a workshop that was co-sponsored by ESF COST Action ES0801, "The ocean chemistry of bioactive trace elements and paleoproxies". Additional support for the workshop came from SCOR, through support to SCOR from the U.S. National Science Foundation (Grant OCE- 0938349 and OCE-1243377) and through a U.S. NSF award to the US GEOTRACES project office (OCE- 0850963). Additional support was from U.S. NSF grant OCE-0963026 to PJL and OCE-0928289 to BST.

## Tables

Table 1. A summary of X-ray based spectroscopic techniques for the analysis of marine particles

| Technique | Sample preparation | Mode of excitation | Measured parameter | Notes | Information obtained |
|---|---|---|---|---|---|
| Scanning Electron Microscopy—Energy-Dispersive Spectrometry (SEM-EDS) | Particles on membrane filter | Benchtop-generated electrons | Elemental X-ray fluorescence | Incident electron beam probes surface (few µm) | Surface morphology and elemental concentration maps (~5 µm spatial resolution) |
| Energy Dispersive X-Ray Fluorescence (EDXRF) | Particles on membrane filter | Benchtop-generated X-rays | Elemental X-ray fluorescence | Incident (hard) X-rays penetrate entire sample | Elemental concentration (bulk) |
| Synchrotron X-Ray Fluorescence (SXRF) | Particles on C-coated EM grid Or particles on membrane filter for coarser mapping | Synchrotron-generated X-rays (Hard X-rays) | Elemental X-ray fluorescence map | Incident (hard) X-rays penetrate entire sample | Elemental concentration maps (submicron to micron spatial resolution) |
| X-ray Absorption Near-Edge Structure (XANES) | Particles on membrane filter | Synchrotron-generated X-rays | X-ray absorption spectrum | Fast (<20 minutes/sample), but not very detailed | Chemical bonding environment of target element and oxidation state, broad groups of chemical species (bulk or microfocused) |
| Extended X-ray Absorption Fine Structure (EXAFS) | Particles on membrane filter | Synchrotron-generated X-rays | X-ray absorption spectrum | Detailed information, but very long analysis time (~8 hrs/sample) | Detailed chemical bonding environment of target element (bulk or microfocused) |
| Scanning Transmission X-ray Microscopy (STXM) | Particles on X-ray transparent substrate such as C-coated EM grid or Si-Ni window | Synchrotron-generated X-rays (soft X-rays only: <2 keV) | Elemental X-ray absorption and X-ray absorption spectrum | Samples must be very thin (transparent to soft X-rays) | Elemental concentration and speciation maps (tens of nm spatial resolution) |
| X-ray Photoelectron Spectroscopy (XPS) | Solids | Benchtop-generated X-rays Synchrotron generated X-rays | Number and kinetic energy of ejected photoelectrons | Surface (10 nm) technique ; detection limit of 0.1% atom number | Elemental concentration and speciation of particle surfaces |

647

**Figure Captions**

Figure 1. Principles of X-ray fluorescence (XRF). Incident X-ray radiation (hν, green squiggly arrow) is absorbed by the target atom, ejecting a (photo)electron (black circle) from the innermost orbital, or shell (short horizontal lines). An electron from an outer shell fills the hole (open circle), emitting fluorescent radiation (hν', red squiggly arrow) at a lower energy, which is detected by a fluorescence detector. The energy of the emitted fluorescent X-ray is element-specific, and is the basis of XRF techniques to determine elemental concentrations (EDXRF, SXRF). SEM-EDS follows the same principles, except that an incident electron beam is used instead of X-rays to excite a core electron. Figure taken from Wikimedia Commons.

Figure 2. Example X-ray absorption spectra for marine particulate iron at a) the $L_3$-edge and b) the K-edge, showing the absorption of X-rays by iron in the sample as a function of incident X-ray energy. The highest absorption (the "absorption edge") occurs when the incident energy equals the binding energies of core electrons, which is around 710 eV for $2p_{3/2}$ electrons ($L_3$-edge) and around 7125 eV for 1s electrons (K-edge). The exact position (energy) of the absorption edge is a function of the oxidation state of the element in the sample (higher energy for more oxidized elements). The edge region is often referred to as the NEXAFS region for soft (lower energy) X-rays, and the XANES region for hard (higher energy) X-rays, but the two terms are equivalent. At energies above the main edge (the EXAFS region), the ejected photoelectron wave is backscattered from surrounding atoms, modulating the absorption probability of incident X-rays. The resulting oscillations in absorption are used to determine the local bonding structure of the central absorber atom. Iron L-edge and K-edge XAS data were collected at beamlines 11.0.2 and 10.3.2, respectively, at the Advanced Light Source, Lawrence Berkeley National Laboratory.

**Figures**

Figure 1.

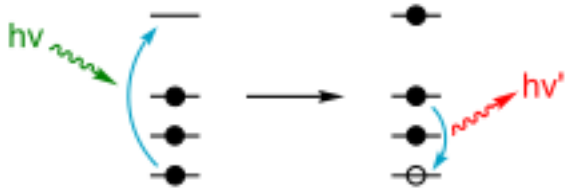


Figure 2.

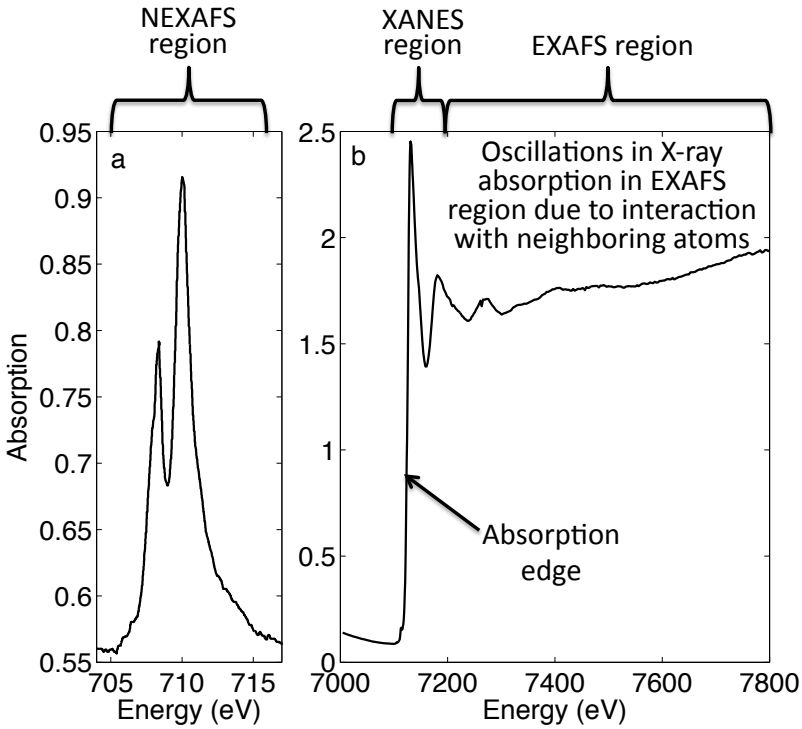

## References


Akagi, T., Fu, F.-f., Hongo, Y., Takahashi, K., 2011. Composition of rare earth elements in settling particles collected in the highly productive North Pacific Ocean and Bering Sea: Implications for siliceous-matter dissolution kinetics and formation of two REE-enriched phases. Geochimica Et Cosmochimica Acta, 75, 4857-4876.

Almeida, S.M., Freitas, M.C., Reis, M., Pinheiro, T., Felix, P.M., Pio, C.A., 2013. Fifteen years of nuclear techniques application to suspended particulate matter studies. Journal of Radioanalytical and Nuclear Chemistry, 297, 347-356.

Anderson, R.F., Fleisher, M.Q., Robinson, L.F., Edwards, L., Hoff, J.A., Moran, S.B., Rutgers vd Loeff, M., Thomas, A., Roy-Barman, M., François, R., 2012. GEOTRACES Intercalibration of $^{230}$Th, $^{232}$Th, $^{231}$Pa and prospects for $^{10}$Be. Limnology and Oceanography: Methods, 10, 179-213.

Baker, E.T., Piper, D.Z., 1976. Suspended particulate matter: collection by pressure filtration and elemental analysis by thin-film X-ray fluorescence. Deep Sea Research and Oceanographic Abstracts, 23, 181-186.

Barrett, P.M., Resing, J.A., Buck, N.J., Buck, C.S., Landing, W.M., Measures, C.I., 2012. The trace element composition of suspended particulate matter in the upper 1000 m of the eastern North Atlantic Ocean: A16N. Marine Chemistry, 142–144, 41-53.

Bates, N.R., Mathis, J.T., 2009. The Arctic Ocean marine carbon cycle: evaluation of air-sea CO2 exchanges, ocean acidification impacts and potential feedbacks. Biogeosciences, 6, 2433-2459.

Behra, P., Bonnissel-Gissinger, P., Alnot, M., Revel, R., Ehrhardt, J.J., 2001. XPS and XAS study of the sorption of Hg(II) onto pyrite. Langmuir, 17, 3970-3979.

Berger, C.J.M., Lippiatt, S.M., Lawrence, M.G., Bruland, K.W., 2008. Application of a chemical leach technique for estimating labile particulate aluminum, iron, and manganese in the Columbia River plume and coastal waters off Oregon and Washington. J. Geophys. Res., 113, C00B01.

Bertin, E.P., 1975. Principles and practice of x-ray spectrometric analysis, 2nd edition. New York: Plenum Press.

Biscaye, P.E., Eittreim, S.L., 1977. Suspended particulate loads and transports in the nepheloid layer of the abyssal Atlantic Ocean. Marine Geology, 23, 155-172.

Bishop, J.K., 1991. Getting good weight. Geophysical Monograph Series, 63, 229-234.

Bishop, J.K.B., 1988. The Barite-Opal-Organic Carbon Association in Oceanic Particulate Matter. Nature, 332, 341-343.

Bishop, J.K.B., Biscaye, P.E., 1982. Chemical characterization of individual particles from the nepheloid layer in the Atlantic Ocean. Earth and Planetary Science Letters, 58, 265-275.

Bishop, J.K.B., Edmond, J.M., Ketten, D.R., Bacon, M.P., Silker, W.B., 1977. Chemistry, Biology, and Vertical Flux of Particulate Matter from Upper 400 M of Equatorial Atlantic Ocean. Deep-Sea Research, 24, 511-548.

Bishop, J.K.B., Lam, P.J., Wood, T.J., 2012. Getting good particles: accurate sampling of particles by large volume in-situ filtration. Limnology and Oceanography Methods, 10, 681-710.

Bishop, J.K.B., Schupack, D., Sherrell, R.M., Conte, M., 1985. A Multiple-Unit Large-Volume In-situ Filtration System for Sampling Oceanic Particulate Matter in Mesoscale Environments. Advances in Chemistry Series, 155-175.

Bluhm, H., Andersson, K., Araki, T., Benzerara, K., Brown, G.E., Dynes, J.J., Ghosal, S., Gilles, M.K., Hansen, H.C., Hemminger, J.C., Hitchcock, A.P., Ketteler, G., Kilcoyne, A.L.D., Kneedler, E., Lawrence, J.R., Leppard, G.G., Majzlam, J., Mun, B.S., Myneni, S.C.B., Nilsson, A., Ogasawara, H., Ogletree, D.F., Pecher, K., Salmeron, M., Shuh, D.K., Tonner, B., Tyliszczak, T., Warwick, T., Yoon, T.H., 2006. Soft X-ray microscopy and spectroscopy at the molecular environmental science beamline at the Advanced Light Source. Journal of Electron Spectroscopy and Related Phenomena, 150, 86-104.

741 Boss, E., Guidi, L., Richardson, M.J., Stemmann, L., Gardner, W., Bishop, J.K.B., Anderson,
742 R.F., Sherrell, R.M., this issue. Optical techniques for in-situ characterization of
743 particles pertinent to GEOTRACES. Progress in Oceanography.
744 Bowie, A.R., Townsend, A.T., Lannuzel, D., Remenyi, T.A., van der Merwe, P., 2010. Modern
745 sampling and analytical methods for the determination of trace elements in marine
746 particulate material using magnetic sector inductively coupled plasma–mass
747 spectrometry. Analytica Chimica Acta, 676, 15-27.
748 Brandes, J.A., Lee, C., Wakeham, S., Peterson, M., Jacobsen, C., Wirick, S., Cody, G.,
749 2004. Examining marine particulate organic matter at sub-micron scales using
750 scanning transmission X-ray microscopy and carbon X-ray absorption near edge
751 structure spectroscopy. Marine Chemistry, 92, 107-121.
752 Breier, J.A., Toner, B.M., Fakra, S.C., Marcus, M.A., White, S.N., Thurnherr, A.M., German,
753 C.R., 2012. Sulfur, sulfides, oxides and organic matter aggregated in submarine
754 hydrothermal plumes at 9°50′N East Pacific Rise. Geochimica Et Cosmochimica Acta,
755 88, 216-236.
756 Brewer, P.G., Nozaki, Y., Spencer, D.W., Fleer, A.P., 1980. Sediment trap experiments in the
757 deep north Atlantic: isotopic and elemental fluxes. Journal Name: J. Mar. Res.;
758 (United States); Journal Volume: 38:4, Medium: X; Size: Pages: 703-728.
759 Brown Jr, G.E., Calas, G., 2012. Mineral-Aqueous Solution Interfaces and Their Impact on
760 the Environment. Geochemical Perspectives, 1, 483-742.
761 Buck, C.S., Landing, W.M., Resing, J., 2013. Pacific Ocean aerosols: Deposition and
762 solubility of iron, aluminum, and other trace elements. Marine Chemistry, 157, 117-
763 130.
764 Buck, C.S., Landing, W.M., Resing, J.A., 2010a. Particle size and aerosol iron solubility: A
765 high-resolution analysis of Atlantic aerosols. Marine Chemistry, 120, 14-24.
766 Buck, C.S., Landing, W.M., Resing, J.A., Lebon, G.T., 2006. Aerosol iron and aluminum
767 solubility in the northwest Pacific Ocean: Results from the 2002 IOC cruise.
768 Geochemistry Geophysics Geosystems, 7.
769 Buck, C.S., Landing, W.M., Resing, J.A., Measures, C.I., 2010b. The solubility and deposition
770 of aerosol Fe and other trace elements in the North Atlantic Ocean: Observations
771 from the A16N CLIVAR/CO2 repeat hydrography section. Marine Chemistry, 120, 57-
772 70.
773 Bunker, G., 2010. Introduction to XAFS: a practical guide to X-ray absorption fine structure
774 spectroscopy: Cambridge University Press.
775 Castruita, M., Saito, M., Schottel, P.C., Elmegreen, L.A., Myneni, S., Stiefel, E.I., Morel,
776 F.M.M., 2006. Overexpression and characterization of an iron storage and DNA-
777 binding Dps protein from Trichodesmium erythraeum. Applied and Environmental
778 Microbiology, 72, 2918-2924.
779 Chase, Z., Anderson, R.F., Fleisher, M.Q., Kubik, P.W., 2002. The influence of particle
780 composition and particle flux on scavenging of Th, Pa and Be in the ocean. Earth and
781 Planetary Science Letters, 204, 215-229.
782 Chester, R., Hughes, M.J., 1967. A chemical technique for the separation of ferro-
783 manganese minerals, carbonate minerals and adsorbed trace elements from pelagic
784 sediments. Chemical Geology, 2, 249-262.
785 Chin, W.-C., Orellana, M.V., Verdugo, P., 1998. Spontaneous assembly of marine dissolved
786 organic matter into polymer gels. Nature, 391, 568-572.
787 Chuang, C.-Y., Santschi, P.H., Ho, Y.-F., Conte, M.H., Guo, L., Schumann, D., Ayranov, M.,
788 Li, Y.-H., 2013. Role of biopolymers as major carrier phases of Th, Pa, Pb, Po, and
789 Be radionuclides in settling particles from the Atlantic Ocean. Marine Chemistry, 157,
790 131-143.
791 Chuang, C.-Y., Santschi, P.H., Jiang, Y., Ho, Y.-F., Quigg, A., Guo, L., Ayranov, M.,
792 Schumann, D., 2014. Important role of biomolecules from diatoms in the scavenging
793 of particle-reactive radionuclides of thorium, protactinium, lead, polonium and
794 beryllium in the ocean: a case study with Phaeodactylum tricornutum. Limnol.
795 Oceanogr., 59, 1256-1266.

796 Collier, R., Edmond, J., 1984. The Trace-Element Geochemistry of Marine Biogenic
797 Particulate Matter. Progress in Oceanography, 13, 113-199.
798 Conradson, S.D., 1998. Application of X-ray absorption fine structure spectroscopy to
799 materials and environmental science. Applied Spectroscopy, 52, 252a-279a.
800 Cowen, J.P., Massoth, G.J., Feely, R.A., 1990. Scavenging rates of dissolved manganese in
801 a hydrothermal vent plume. Deep Sea Research Part A. Oceanographic Research
802 Papers, 37, 1619-1637.
803 Criss, J.W., 1976. Particle size and composition effects in x-ray fluorescence analysis of
804 pollution samples. Analytical Chemistry, 48, 179-186.
805 Cullen, J.T., Field, M.P., Sherrell, R.M., 2001. Determination of trace elements in filtered
806 suspended marine particulate material by sector field HR-ICP-MS. Journal of
807 Analytical Atomic Spectrometry, 16, 1307-1312.
808 Cullen, J.T., Sherrell, R.M., 1999. Techniques for determination of trace metals in small
809 samples of size-fractionated particulate matter: phytoplankton metals off central
810 California. Marine Chemistry, 67, 233-247.
811 Dehairs, F., Chesselet, R., Jedwab, J., 1980. Discrete suspended particles of barite and the
812 barium cycle in the open ocean. Earth and Planetary Science Letters, 49, 528-550.
813 DeMaster, D.J., 1981. The supply and accumulation of silica in the marine environment.
814 Geochimica Et Cosmochimica Acta, 45, 1715-1732.
815 Deuser, W.G., Ross, E.H., Anderson, R.F., 1981. Seasonality in the supply of sediment to
816 the deep Sargasso Sea and implications for the rapid transfer of matter to the deep
817 ocean. Deep-Sea Research Part a-Oceanographic Research Papers, 28, 495-505.
818 Dieckmann, G.S., Nehrke, G., Papadimitriou, S., Göttlicher, J., Steininger, R., Kennedy, H.,
819 Wolf-Gladrow, D., Thomas, D.N., 2008. Calcium carbonate as ikaite crystals in
820 Antarctic sea ice. Geophysical Research Letters, 35, L08501.
821 Duckworth, O.W., Bargar, J.R., Sposito, G., 2008. Sorption of ferric iron from ferrioxamine B
822 to synthetic and biogenic layer type manganese oxides. Geochimica Et
823 Cosmochimica Acta, 72, 3371-3380.
824 Dymond, J., Suess, E., Lyle, M., 1992. Barium in Deep-Sea Sediment: A Geochemical Proxy
825 for Paleoproductivity. Paleoceanography, 7, 163-181.
826 Dzubay, T.G., Nelson, R.O., 1975. Self Absorption Corrections for X-Ray Fluorescence
827 Analysis of Aerosols. In W. Pickles, C. Barrett, J. Newkirk, C. Ruud (Eds.), Advances
828 in X-Ray Analysis (pp. 619-631): Springer US.
829 Feely, R.A., Massoth, G.J., Lebon, G.T., 1991a. Sampling of Marine Particulate Matter and
830 Analysis by X−Ray Fluorescence Spectrometry. Marine particles: analysis and
831 characterization, 251-257.
832 Feely, R.A., Trefry, J.H., Lebon, G.T., German, C.R., 1998. The relationship between P/Fe
833 and V/Fe ratios in hydrothermal precipitates and dissolved phosphate in seawater.
834 Geophys. Res. Lett., 25, 2253-2256.
835 Feely, R.A., Trefry, J.H., Massoth, G.J., Metz, S., 1991b. A comparison of the scavenging of
836 phosphorus and arsenic from seawater by hydrothermal iron oxyhydroxides in the
837 Atlantic and Pacific Oceans. Deep Sea Research Part A. Oceanographic Research
838 Papers, 38, 617-623.
839 Feldmann, I., Tittes, W., Jakubowski, N., Stuewer, D., Giessmann, U., 1994. Performance
840 Characteristics of Inductively-Coupled-Plasma Mass Spectrometry with High-Mass
841 Resolution. Journal of Analytical Atomic Spectrometry, 9, 1007-1014.
842 Fenter, P., Rivers, M., Sturchio, N., Sutton, S., (Eds.), 2002. Applications of synchrotron
843 radiation in low-temperature geochemistry and environmental sciences.: Geochemical
844 Society.
845 Fleer, A.P., Bacon, M.P., 1991. Notes on some techniques of marine particle analysis used
846 at WHOI In D.C. Hurd, D.W. Spencer (Eds.), Marine Particles : Analysis and
847 Characterization (pp. 223-226): American Geophysical Union.
848 François, R., Honjo, S., Krishfield, R., Manganini, S., 2002. Factors controlling the flux of
849 organic carbon to the bathypelagic zone of the ocean. Global Biogeochemical Cycles,
850 16.

Goldberg, E.D., 1954. Marine geochemistry 1. Chemical scavengers of the sea. The Journal of Geology, 249-265.
Goldstein, J., Newbury, D.E., Joy, D.C., Lyman, C.E., Echlin, P., Lifshin, E., Sawyer, L., Michael, J.R., 2003. Scanning electron microscopy and X-ray microanalysis: Springer.
Heldal, M., Fagerbakke, K., Tuomi, P., Bratbak, G., 1996. Abundant populations of iron and manganese sequestering bacteria in coastal water. Aquatic Microbial Ecology, 11, 127-133.
Heldal, M., Scanlan, D.J., Norland, S., Thingstad, F., Mann, N.H., 2003. Elemental Composition of Single Cells of Various Strains of Marine Prochlorococcus and Synechococcus Using X-Ray Microanalysis. Limnology and Oceanography, 48, 1732-1743.
Ho, T.Y., Chou, W.C., Lin, H.L., Sheu, D.D., 2011. Trace metal cycling in the deep water of the South China Sea: The composition, sources, and fluxes of sinking particles. Limnology and Oceanography, 56, 1225-1243.
Ho, T.Y., Chou, W.C., Wei, C.L., Lin, F.J., Wong, G.T.F., Lin, H.L., 2010. Trace metal cycling in the surface water of the South China Sea: Vertical fluxes, composition, and sources. Limnology and Oceanography, 55, 1807-1820.
Ho, T.Y., Wen, L.S., You, C.F., Lee, D.C., 2007. The trace-metal composition of size-fractionated plankton in the South China Sea: Biotic versus abiotic sources. Limnology and Oceanography, 52, 1776-1788.
Hołyńska, B., Bisiniek, K., 1976. Determination of trace amounts of metals in saline water by energy dispersive XRF using the NaDDTC preconcentration. Journal of Radioanalytical Chemistry, 31, 159-166.
Honjo, S., Dymond, J., Collier, R., Manganini, S.J., 1995. Export Production of Particles to the Interior of the Equatorial Pacific-Ocean During the 1992 Eqpac Experiment. Deep-Sea Research Part Ii-Topical Studies in Oceanography, 42, 831-870.
Hurd, D.C., Spencer, D.W., 1991. Marine particles: analysis and characterization: American Geophysical Union.
Ingall, E.D., Diaz, J.M., Longo, A.F., Oakes, M., Finney, L., Vogt, S., Lai, B., Yager, P.L., Twining, B.S., Brandes, J.A., 2013. Role of biogenic silica in the removal of iron from the Antarctic seas. Nature communications, 4.
Jeandel, C., Rutgers van der Loeff, M., Lam, P.J., Roy-Barman, M., Sherrell, R.M., Kretschmer, S., German, C.R., Dehairs, F., this issue. What did we learn about the oceanic particle dynamics from the GEOSECS-JGOFS era? Progress in Oceanography.
Karageorgis, A.P., Gardner, W.D., Georgopoulos, D., Mishonov, A.V., Krasakopoulou, E., Anagnostou, C., 2008. Particle dynamics in the Eastern Mediterranean Sea: A synthesis based on light transmission, PMC, and POC archives (1991–2001). Deep Sea Research Part I: Oceanographic Research Papers, 55, 177-202.
Kelly, S., Hesterberg, D., Ravel, B., 2008. Analysis of soils and minerals using X-ray absorption spectroscopy. Methods of soil analysis. Part, 5, 387-463.
Kheboian, C., Bauer, C.F., 1987. Accuracy of selective extraction procedures for metal speciation in model aquatic sediments. Analytical Chemistry, 59, 1417-1423.
King, A.L., Sanudo-Wilhelmy, S.A., Boyd, P.W., Twining, B.S., Wilhelm, S.W., Breene, C., Ellwood, M.J., Hutchins, D.A., 2012. A comparison of biogenic iron quotas during a diatom spring bloom using multiple approaches. Biogeosciences, 9, 667-687.
Klaas, C., Archer, D.E., 2002. Association of sinking organic matter with various types of mineral ballast in the deep sea: Implications for the rain ratio. Global Biogeochemical Cycles, 16, 1116-1129.
Koningsberger, D., Prins, R., 1988. X-ray absorption: principles, applications, techniques of EXAFS, SEXAFS, and XANES.
Kuss, J., Kremling, K., 1999. Spatial variability of particle associated trace elements in near-surface waters of the North Atlantic (30 degrees N/60 degrees W to 60 degrees N/2 degrees W), derived by large-volume sampling. Marine Chemistry, 68, 71-86.

906 Lam, P.J., Bishop, J.K.B., 2007. High Biomass Low Export regimes in the Southern Ocean.
907 Deep Sea Research Part II: Topical Studies in Oceanography, 54, 601-638.
908 Lam, P.J., Bishop, J.K.B., 2008. The continental margin is a key source of iron to the HNLC
909 North Pacific Ocean. Geophysical Research Letters, 35, L07608.
910 Lam, P.J., Bishop, J.K.B., Henning, C.C., Marcus, M.A., Waychunas, G.A., Fung, I.Y., 2006.
911 Wintertime phytoplankton bloom in the subarctic Pacific supported by continental
912 margin iron. Global Biogeochemical Cycles, 20, doi:10.1029/2005GB002557.
913 Lam, P.J., Morris, P.J., Patent pending. In situ marine sample collection system and
914 methods. Application No. 13/864,655.
915 Lam, P.J., Ohnemus, D.C., Auro, M.E., in press. Size fractionated major particle composition
916 and mass from the US GEOTRACES North Atlantic Zonal Transect. Deep Sea
917 Research Part II: Topical Studies in Oceanography.
918 Lam, P.J., Ohnemus, D.C., Marcus, M.A., 2012. The speciation of marine particulate iron
919 adjacent to active and passive continental margins. Geochimica Et Cosmochimica
920 Acta, 80, 108-124.
921 Lamborg, C.H., Buesseler, K.O., Lam, P.J., 2008. Sinking fluxes of minor and trace elements
922 in the North Pacific Ocean measured during the VERTIGO program. Deep-Sea
923 Research Part Ii-Topical Studies in Oceanography, 55, 1564-1577.
924 Landing, W.M., Bruland, K.W., 1987. The Contrasting Biogeochemistry of Iron and
925 Manganese in the Pacific-Ocean. Geochimica Et Cosmochimica Acta, 51, 29-43.
926 Lavoie, D.M., 1992. Computerized oceanic particle characterization using heavy metal
927 staining, SEM, EDXS and image analysis. Deep Sea Research Part A.
928 Oceanographic Research Papers, 39, 1655-1668.
929 Lehmann, J., Solomon, D., Brandes, J., Fleckenstein, H., Jacobsen, C., Thieme, J., 2009.
930 Synchrotron-based near-edge X-ray spectroscopy of natural organic matter in soils
931 and sediments. Biophysico-Chemical Processes Involving Natural Nonliving Organic
932 Matter in Environmental Systems, 729-781.
933 Linge, K.L., Jarvis, K.E., 2009. Quadrupole ICP-MS: Introduction to Instrumentation,
934 Measurement Techniques and Analytical Capabilities. Geostandards and
935 Geoanalytical Research, 33, 445-467.
936 Manceau, A., Drits, V., 1993. Local structure of ferrihydrite and feroxyhite by EXAFS
937 spectroscopy. Clay Minerals, 28, 165-165.
938 Marcus, M.A., 2011. The Linear Fit Programs. xraysweb.lbl.gov: LBL.
939 Marcus, M.A., Manceau, A., Kersten, M., 2004. Mn, Fe, Zn and As speciation in a fast-
940 growing ferromanganese marine nodule. Geochimica Et Cosmochimica Acta, 68,
941 3125-3136.
942 Marcus, M.A., Westphal, A.J., Fakra, S.C., 2008. Classification of Fe-bearing species from K-
943 edge XANES data using two-parameter correlation plots. Journal of Synchrotron
944 Radiation, 15, 463-468.
945 Martin, J.H., Knauer, G.A., 1973. Elemental Composition of Plankton. Geochimica Et
946 Cosmochimica Acta, 37, 1639-1653.
947 McDonnell, A.M.P., Lam, P.J., Lamborg, C.H., Buesseler, K.O., Sanders, R., Riley, J.S.,
948 Marsay, C., Smith, H.E.K., Sargent, E.C., Lampitt, R.S., Bishop, J.K.B., this issue.
949 The oceanographic toolbox for the collection of sinking and suspended marine
950 particles. Progress in Oceanography.
951 Mortlock, R.A., Froelich, P.N., 1989. A Simple Method for the Rapid-Determination of
952 Biogenic Opal in Pelagic Marine-Sediments. Deep-Sea Research Part a-
953 Oceanographic Research Papers, 36, 1415-1426.
954 Newville, M., 2004. Fundamentals of XAFS. External link:
955 http://xafs.org/Tutorials?action=AttachFile&do=get&target=Newville_xas_fundamental
956 s.pdf.
957 Nirel, P.M.V., Morel, F.M.M., 1990. Pitfalls of Sequential Extractions. Water Research, 24,
958 1055-1056.
959 Nuester, J., Newville, M., Twining, B.S., 2014. Distributions of iron, phosphorus and sulfur
960 along trichomes of the cyanobacteria Trichodesmium. Metallomics, 6, 1141-1149.

961 Nuester, J., Vogt, S., Newville, M., Kustka, A.B., Twining, B.S., 2012. The unique
962 biogeochemical signature of the marine diazotroph Trichodesmium. Frontiers in
963 Microbiology, 3.
964 Núnez-Milland, D.R., Baines, S.B., Vogt, S., Twining, B.S., 2010. Quantification of
965 phosphorus in single cells using synchrotron X-ray fluorescence. Journal of
966 Synchrotron Radiation, 17, 560-566.
967 Ohnemus, D.C., Lam, P.J., in press. Cycling of Lithogenic Marine Particulates in the US
968 GEOTRACES North Atlantic Zonal Transect. Deep-Sea Research II.
969 Ohnemus, D.C., Sherrell, R.M., Lagerstöm, M., Morton, P.L., Twining, B.S., Rauschenberg,
970 S.M., Auro, M.E., Lam, P.J., 2014. Piranha: a chemical method for dissolution of
971 polyethersulfone filters and laboratory inter-comparison of marine particulate digests.
972 Limnology and Oceanography: Methods, 12, 530-547.
973 Parsons, J.G., Aldrich, M.V., Gardea-Torresdey, J.L., 2002. Environmental and biological
974 applications of extended X-ray absorption fine structure (EXAFS) and X-ray
975 absorption near edge structure (XANES) spectroscopies. Applied Spectroscopy
976 Reviews, 37, 187-222.
977 Planquette, H., Sherrell, R.M., 2012. Sampling for particulate trace element determination
978 using water sampling bottles: methodology and comparison to in situ pumps. Limnol.
979 Oceanogr.: Methods, 10, 367-388.
980 Quigley, M.S., Santschi, P.H., Hung, C.C., Guo, L.D., Honeyman, B.D., 2002. Importance of
981 acid polysaccharides for Th-234 complexation to marine organic matter. Limnology
982 and Oceanography, 47, 367-377.
983 Ragueneau, O., Savoye, N., Del Amo, Y., Cotten, J., Tardiveau, B., Leynaert, A., 2005. A
984 new method for the measurement of biogenic silica in suspended matter of coastal
985 waters: using Si:Al ratios to correct for the mineral interference. Continental Shelf
986 Research, 25, 697-710.
987 Ranville, M.A., Cutter, G.A., Buck, C.S., Landing, W.M., Cutter, L.S., Resing, J.A., Flegal,
988 A.R., 2010. Aeolian Contamination of Se and Ag in the North Pacific from Asian
989 Fossil Fuel Combustion. Environmental Science & Technology, 44, 1587-1593.
990 Ravel, B., Newville, M., 2005. ATHENA, ARTEMIS, HEPHAESTUS: data analysis for X-ray
991 absorption spectroscopy using IFEFFIT. Journal of Synchrotron Radiation, 12, 537-
992 541.
993 Resing, J., Lebon, G., Baker, E., Lupton, J., Embley, R., Massoth, G., Chadwick, W., De
994 Ronde, C., 2007. Venting of acid-sulfate fluids in a high-sulfidation setting at NW
995 Rota-1 submarine volcano on the Mariana Arc. Economic Geology, 102, 1047-1061.
996 Roberts, K.A., Xu, C., Hung, C.-C., Conte, M.H., Santschi, P.H., 2009. Scavenging and
997 fractionation of thorium vs. protactinium in the ocean, as determined from particle–
998 water partitioning experiments with sediment trap material from the Gulf of Mexico
999 and Sargasso Sea. Earth and Planetary Science Letters, 286, 131-138.
1000 Robin, E., Rabouille, C., Martinez, G., Lefevre, I., Reyss, J., Van Beek, P., Jeandel, C., 2003.
1001 Direct barite determination using SEM/EDS-ACC system: implication for constraining
1002 barium carriers and barite preservation in marine sediments. Marine Chemistry, 82,
1003 289-306.
1004 Roy-Barman, M., Jeandel, C., Souhaut, M., Rutgers van der Loeff, M., Voege, I., Leblond, N.,
1005 Freydier, R., 2005. The influence of particle composition on thorium scavenging in the
1006 NE Atlantic ocean (POMME experiment). Earth and Planetary Science Letters, 240,
1007 681-693.
1008 Sandroni, V., Smith, C.M.M., 2002. Microwave digestion of sludge, soil and sediment
1009 samples for metal analysis by inductively coupled plasma-atomic emission
1010 spectrometry. Analytica Chimica Acta, 468, 335-344.
1011 Sham, T., Rivers, M.L., 2002. A brief overview of synchrotron radiation. Reviews in
1012 Mineralogy and Geochemistry, 49, 117-147.
1013 Sherrell, R.M., Boyle, E.A., 1992. The Trace-Metal Composition of Suspended Particles in
1014 the Oceanic Water Column near Bermuda. Earth and Planetary Science Letters, 111,
1015 155-174.

1016 Sholkovitz, E.R., 1989. Artifacts associated with the chemical leaching of sediments for rare-
1017 earth elements. Chemical Geology, 77, 47-51.
1018 Spencer, D.W., Brewer, P.G., Fleer, A., Honjo, S., Krishnaswami, S., Nozaki, Y., 1978.
1019 Chemical fluxes from a sediment trap experiment in deep Sargasso Sea. Journal of
1020 Marine Research, 36, 493-523.
1021 Spencer, D.W., Sachs, P.L., Brewer, P.G., 1972. Aspects of the distribution and trace
1022 element composition of suspended matter in the Black Sea. Geochimica Et
1023 Cosmochimica Acta, 36, 71-86.
1024 Steinnes, E., 2000. Neutron activation techniques in environmental studies. Journal of
1025 Radioanalytical and Nuclear Chemistry, 243, 235-239.
1026 Sternberg, E., Jeandel, C., Robin, E., Souhaut, M., 2008. Seasonal cycle of suspended barite
1027 in the mediterranean sea. Geochimica Et Cosmochimica Acta, 72, 4020-4034.
1028 Tamura, N., Celestre, R.S., MacDowell, A.A., Padmore, H.A., Spolenak, R., Valek, B.C.,
1029 Meier Chang, N., Manceau, A., Patel, J.R., 2002. Submicron x-ray diffraction and its
1030 applications to problems in materials and environmental science. Review of Scientific
1031 Instruments, 73, 1369-1372.
1032 Tang, D., Morel, F.M.M., 2006. Distinguishing between cellular and Fe-oxide-associated
1033 trace elements in phytoplankton. Marine Chemistry, 98, 18-30.
1034 Teo, B.K., 1986. EXAFS: basic principles and data analysis: Springer-Verlag Berlin.
1035 Tessier, A., Campbell, P.G.C., Bisson, M., 1979. Sequential extraction procedure for the
1036 speciation of particulate trace metals. Analytical Chemistry, 51, 844-851.
1037 Timothy, D.A., Soon, M.Y.S., Calvert, S.E., 2003. Settling fluxes in Saanich and Jervis Inlets,
1038 British Columbia, Canada: sources and seasonal patterns. Progress in
1039 Oceanography, 59, 31-73.
1040 Toner, B.M., BerquÛ, T.S., Michel, F.M., Sorensen, J.V., Templeton, A.S., Edwards, K.J.,
1041 2012a. Mineralogy of iron microbial mats from Loihi Seamount. Frontiers in
1042 Microbiology, 3.
1043 Toner, B.M., Fakra, S.C., Manganini, S.J., Santelli, C.M., Marcus, M.A., Moffett, J., Rouxel,
1044 O., German, C.R., Edwards, K.J., 2009a. Preservation of iron(II) by carbon-rich
1045 matrices in a hydrothermal plume. Nature Geoscience, 2, 197-201.
1046 Toner, B.M., Marcus, M.A., Edwards, K.J., Rouxel, O., German, C.R., 2012b. Measuring the
1047 Form of Iron in Hydrothermal Plume Particles. Oceanography, 25, 209-212.
1048 Toner, B.M., Nicholas, S.L., Wasik, J.K.C., 2014. Scaling up: fulfilling the promise of X-ray
1049 microprobe for biogeochemical research. Environmental Chemistry, 11, 4-9.
1050 Toner, B.M., Santelli, C.M., Marcus, M.A., Wirth, R., Chan, C.S., McCollom, T., Bach, W.,
1051 Edwards, K.J., 2009b. Biogenic iron oxyhydroxide formation at mid-ocean ridge
1052 hydrothermal vents: Juan de Fuca Ridge. Geochimica Et Cosmochimica Acta, 73,
1053 388-403.
1054 Tovar-Sanchez, A., Sanudo-Wilhelmy, S.A., Garcia-Vargas, M., Weaver, R.S., Popels, L.C.,
1055 Hutchins, D.A., 2003. A trace metal clean reagent to remove surface-bound iron from
1056 marine phytoplankton. Marine Chemistry, 82, 91-99.
1057 Turekian, K.K., 1977. The fate of metals in the oceans. Geochimica Et Cosmochimica Acta,
1058 41, 1139-1144.
1059 Twining, B.S., Baines, S.B., 2013. The Trace Metal Composition of Marine Phytoplankton.
1060 Annual Review of Marine Science, 5, 191-215.
1061 Twining, B.S., Baines, S.B., Bozard, J.B., Vogt, S., Walker, E.A., Nelson, D.M., 2011. Metal
1062 quotas of plankton in the equatorial Pacific Ocean. Deep-Sea Research Part Ii-
1063 Topical Studies in Oceanography, 58, 325-341.
1064 Twining, B.S., Baines, S.B., Fisher, N.S., 2004a. Element stoichiometries of individual
1065 plankton cells collected during the Southern Ocean Iron Experiment (SOFeX).
1066 Limnology and Oceanography, 49, 2115-2128.
1067 Twining, B.S., Baines, S.B., Fisher, N.S., Landry, M.R., 2004b. Cellular iron contents of
1068 plankton during the Southern Ocean Iron Experiment (SOFeX). Deep-Sea Research
1069 Part I-Oceanographic Research Papers, 51, 1827-1850.

Twining, B.S., Baines, S.B., Fisher, N.S., Maser, J., Vogt, S., Jacobsen, C., Tovar-Sanchez, A., Sanudo-Wilhelmy, S.A., 2003. Quantifying trace elements in individual aquatic protist cells with a synchrotron X-ray fluorescence microprobe. Analytical Chemistry, 75, 3806-3816.

Twining, B.S., Baines, S.B., Vogt, S., de Jonge, M.D., 2008. Exploring ocean biogeochemistry by single-cell microprobe analysis of protist elemental composition. Journal of Eukaryotic Microbiology, 55, 151-162.

Twining, B.S., Nuñez-Milland, D., Vogt, S., Johnson, R.S., Sedwick, P.N., 2010. Variations in Synechococcus cell quotas of phosphorus, sulfur, manganese, iron, nickel, and zinc within mesoscale eddies in the Sargasso Sea. Limnology and Oceanography, 55, 492.

Twining, B.S., Rauschenberg, S., Morton, P., Ohnemus, D.C., Lam, P.J., in press. Comparison of particulate trace element concentrations in the North Atlantic Ocean as determined with discrete bottle sampling and in situ pumping. Deep Sea Research Part II: Topical Studies in Oceanography.

Verdugo, P., Santschi, P.H., 2010. Polymer dynamics of DOC networks and gel formation in seawater. Deep Sea Research Part II: Topical Studies in Oceanography, 57, 1486-1493.

von der Heyden, B.P., Hauser, E.J., Mishra, B., Martinez, G.A., Bowie, A.R., Tyliszczak, T., Mtshali, T.N., Roychoudhury, A.N., Myneni, S.C.B., 2014. Ubiquitous Presence of Fe(II) in Aquatic Colloids and Its Association with Organic Carbon. Environmental Science & Technology Letters.

von der Heyden, B.P., Roychoudhury, A.N., Mtshali, T.N., Tyliszczak, T., Myneni, S.C.B., 2012. Chemically and Geographically Distinct Solid-Phase Iron Pools in the Southern Ocean. Science, 338, 1199-1201.

Wasinger, E.C., de Groot, F.M.F., Hedman, B., Hodgson, K.O., Solomon, E.I., 2003. L-edge X-ray Absorption Spectroscopy of Non-Heme Iron Sites: Experimental Determination of Differential Orbital Covalency. Journal of the American Chemical Society, 125, 12894-12906.

Waychunas, G.A., Brown, G.E., Apted, M.J., 1986. X-Ray K-Edge Absorption-Spectra of Fe Minerals and Model Compounds .2. Exafs. Physics and Chemistry of Minerals, 13, 31-47.

Webb, S.M., 2005. SIXpack: a graphical user interface for XAS analysis using IFEFFIT. Physica Scripta, 2005, 1011.

Wilke, M., Farges, F., Petit, P.E., Brown, G.E., Martin, F., 2001. Oxidation state and coordination of Fe in minerals: An FeK-XANES spectroscopic study. American Mineralogist, 86, 714-730.

1108